Biosensors and Bioelectronics 24 (2009) 2250–2254

Contents lists available at ScienceDirect

Biosensors and Bioelectronics

journal homepage: www.elsevier.com/locate/bios

Short communication

Detecting effects of low levels of cytochalasin B in 3T3 fibroblast cultures by analysis of electrical noise obtained from cellular micromotion

Douglas C. Lovelady, Jennifer Friedman, Sonali Patel, David A. Rabson, Chun-Min Lo*

Department of Physics, University of South Florida, Tampa, FL 33620, USA

ARTICLE INFO

Article history:
Received 10 August 2008
Received in revised form
13 September 2008
Accepted 24 September 2008
Available online 17 October 2008

Keywords:
ECIS
Noise analysis
Toxin assay
Cytochalasin B

ABSTRACT

We performed micromotion experiments using electric cell–substrate impedance sensing (ECIS) on a confluent layer of 3T3 fibroblasts exposed to different low levels of the toxin cytochalasin B. This toxin is know to affect actin polymerization and to disrupt cytoskeletal structure and function in cells, changing the morphology of confluent cell cultures and altering the nature of the cellular micromotion, which is measured by ECIS as changes in impedance. By looking at several measures to characterize the long- and short-term correlations in the noise of the impedance time series, we are able to detect the effects of the toxin at concentrations down to 1 μM; there are intriguing hints that the effects may be discernible at levels as low as 0.1 μM. These measures include the power spectrum, the Hurst and detrended-fluctuation-analysis exponents, and the first zero and first $1/e$ crossings of the autocorrelation function. While most published work with ECIS uses only average impedance values, we demonstrate that noise analysis provides a more sensitive probe.

1. Introduction

Impedance measurement through microelectrodes was first used to study the characteristics of anchorage-dependent cultured cell lines by Giaever and Keese Giaever and Keese (1984). They developed a cell-based biosensor, referred to as electric cell–substrate impedance sensing (ECIS), which can be applied to detect subtle changes in cell–substrata interactions, including cell motion. A cell-electrode model of the system developed earlier shows that most of the current flows under or around the cells, while the current flowing through the cells is significant but small in comparison (Giaever and Keese, 1991). Upon the attachment and spreading of cells, the impedance increases, because the cells act as insulating particles to restrict the current. An intriguing feature is the fluctuation in the measured impedance, which is always associated with living cells and persists even if the cell layer becomes fully confluent (Giaever and Keese, 1989). This behavior is attributed to motion or micromotion of the cells, an indication of cell viability and morphology change. When cells are exposed to a cytotoxic compound, the chemical might affect any downstream event in a signaling cascade, resulting in cytoskeletal disruption and reorganization, and then alter cell morphology and motility. In this aspect, cell–cell and cell–substrate interactions measured by ECIS assays can be used as a predictor of cytotoxicity to reflect integrated cellular responses to toxic stimuli (Keese et al., 1998).

The toxin cytochalasin B interferes with cytoskeleton function by inhibiting actin polymerization (Shier and Mebs, 1990; Tanenbaum, 1978; Bonder and Mooseker, 1986; Brown and Spudich, 1981). At sufficiently high concentration, cytochalasin poisoning of cells leads to a number of morphological and functional effects, including arborization, inhibition of endocytosis and secretion, suppression of cytoplasmic division, and enucleation (Shier and Mebs, 1990; Tanenbaum, 1978; Foissner and Wasteneys, 2007; Ohmori et al., 1992). The electrical resistance of a cell culture jumps rapidly with the addition of a low concentration of the toxin to the medium in a flow cell; this jump is reversed just as rapidly when the toxin is flushed (Brischwein et al., 2003). Although such jumps in resistance provide an unmistakable signature for the addition and subsequent elimination of cytochalasin B, the *absolute* resistance gives a far less sensitive signal: given an average resistance over half an hour, one can perhaps distinguish a 2.5- μM concentration in the medium from no toxin, but the correlation between absolute resistance and concentration is too weak for finer comparisons when the experiment does not permit dynamic control over the levels of toxin in the medium.

Although ECIS has found wide application in monitoring cell cultures, in most published ECIS work (*e.g.*, Giaever and Keese, 1984; Lo et al., 1993; Xiao and Luong, 2005; Hartmann et al., 2007; Charrier et al., 2007; Saxena et al., 2007; Earley and Plopper, 2008), only a time-averaged signal, or a secular trend in resistance over many

* Corresponding author. Tel.: +1 813 974 7793; fax: +1 813 974 5813.
E-mail address: cmlo@cas.usf.edu (C.-M. Lo).

0956-5663/$ – see front matter © 2008 Elsevier B.V. All rights reserved.
doi:10.1016/j.bios.2008.09.033

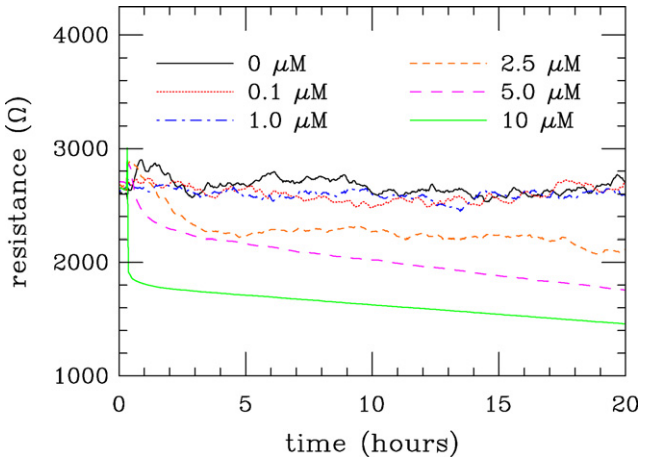

Fig. 1. Displayed is resistance as a function of time in confluent cultures of 3T3 fibroblasts exposed to medium containing the toxin cytochalasin B in concentrations of 0, 0.1, 1.0, 2.5, 5.0, and 10 μM.

hours, is used. We will argue that a statistical analysis of impedance noise does a better job of distinguishing low levels of cytochalasin B in culture than does average impedance.

Fig. 1, plotting resistance against time for six separate cultures, makes clear the inability of averaged resistance to distinguish low levels of toxin. While the three higher concentrations are easily distinguished from the three lowest, one cannot tell the differences among the three lowest concentrations. This is confirmed in Fig. 2, showing that even averaging 5–7 h of data at each concentration (between nine and twelve runs, each of duration 2048 s) cannot distinguish the three lowest toxin levels.

In Lovelady et al. (2007), we introduced a statistical technique for analyzing the rapid and apparently "random" noise fluctuations

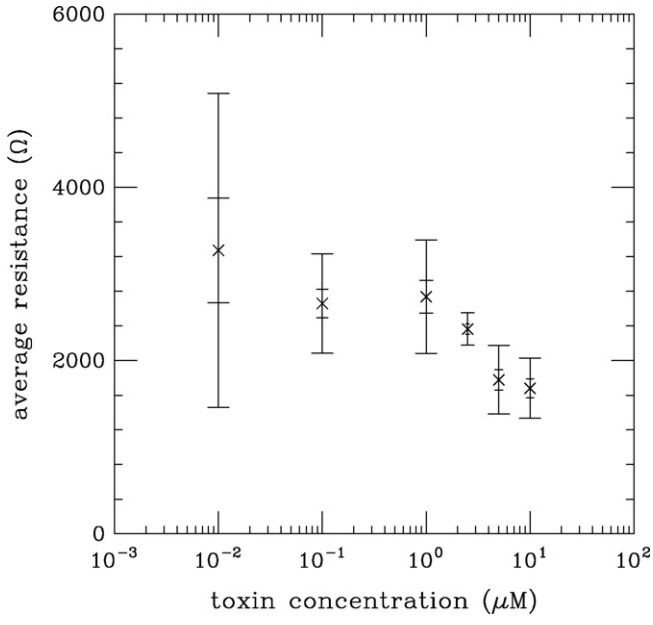

Fig. 2. Average resistances of ECIS runs (as in Fig. 1) do not distinguish low concentrations of cytochalasin B. Symbols (×) plot the averages of multiple runs as functions of concentration; control runs (0 μM) are plotted at 0.01 μM. For each concentration, the outer error bar gives the population standard deviation, the inner error bar the standard error of the mean. The standard errors of the mean of the lowest three concentrations all overlap, consistent with the picture presented in Fig. 1. We averaged nine 2048-s runs at 0 μM, twelve at 0.1 μM, twelve at 1.0 μM, ten at 2.5 μM, eleven at 5.0 μM, and ten at 10 μM.

seen in ECIS experiments and demonstrated that such analysis can distinguish cancerous from non-cancerous cultures of human ovarian surface epithelial cells. We now apply these ideas to cultures of 3T3 fibroblasts with levels of cytochalasin B in the medium ranging from zero to 10 μM and show that the noise spectrum distinguishes different concentrations more effectively than average resistance. As with the previous work, the statistical measures include the power spectrum of the noise, Hurst exponents, detrended fluctuation analysis, and statistical tests of population differences.

2. Experimental

2.1. Cell culture

The 3T3 fibroblasts, obtained from the American Type Culture Collection (Manassas, VA), were grown in DMEM (4.5 g/L D-glucose) (Mediatech, Manassas, VA) supplemented with 10% FBS (Mediatech), 50 μg/mL streptomycin, 50 units/mL penicillin, and 250 ng/mL amphotericin B under 5% CO_2, and a 37°C, high-humidity atmosphere. For ECIS micromotion measurements, cells were harvested and grown to confluence 24 h before addition of cytochalasin B into the electrode wells, resulting in a cell density that was controlled at 10^5 cell/cm^2. Cytochalasin B (Sigma, St. Louis, MO) was diluted in DMSO as a 10-mM solution before use.

2.2. ECIS

We used the ECIS system (from Applied Biophysics, Inc., Troy, NY) to collect micromotion time–series data, the fluctuations in which are caused by the movements in a confluent layer of live cells. The system can be modeled as an RC circuit (Giaever and Keese, 1989, 1991; Lo et al., 1993, 1995). The cells are cultured on a small gold electrode (5×10^{-4} cm^2), which is connected in series to a 1-Megaohm resister, an AC signal generator operating at 1 volt and 4000 Hz, and finally to a large gold counter-electrode (0.15 cm^2). This network is connected in parallel to a lock-in amplifier, and the in-phase and out-of-phase voltages are collected once a second, from which we extract time series of resistance and capacitive reactance. In ECIS experiments, the fluctuations in complex impedance come primarily from changes in intercellular gaps and in the narrow spaces between the cells and the small gold electrode (Giaever and Keese, 1991; Lo et al., 1995, 1993). A current of about one microamp is driven through the sample, and the resulting voltage drop of a few millivolts across the cell layer has no physiological effect: this is a non-invasive, in-vitro technique.

To expose 3T3 cell layers to cytochalasin B, 0.4 mL of complete culture medium was used in each well before adding the cytochalasin B solution. Serial dilutions were prepared in culture medium, and 0.1 mL of toxin solution was carefully added to each well to achieve the final desired concentration. In control experiments, each well received the same amount of culture medium without cytochalasin B. Note that in the ECIS apparatus, the wells are completely independent. We emphasize that we are *not* dynamically changing toxin levels as in flow-cell experiments (Brischwein et al., 2003); to see the effects of the toxin will require statistical analysis.

From 64 separate cultures, we collected time series of which nine were at zero concentration of the toxin cytochalasin B. We took twelve runs at 0.1 μM, twelve at 1.0 μM, ten at 2.5 μM, eleven at 5.0 μM, and ten at 10 μM.[1] Each 2048-s run (just over 1/2 h) was

[1] The equipment accommodates eight independent runs in each experiment, and we chose to run all six concentrations in each experiment; so two concentrations were repeated in each experiment. This accounts for the small differences in numbers of runs. However, these differences do not affect our statistical analysis.

taken 24 h after the introduction of the toxin to ensure that the cells received the full effect at each concentration. We numerically differentiated the resistance and capacitance time series to obtain noise time series for each, which we normalized to zero mean and unit variance.

3. Results

While the power spectrum, Hurst exponent, and detrended fluctuation analysis give us ways of quantifying long-term correlations in the noise, the Fourier transform of the power spectrum yields autocorrelation, which enables us to quantify and study short-term correlations. In what follows we examine the real part of impedance from the experiments. At 4000 Hz, the imaginary or capacitive part was not as useful at distinguishing the different toxins levels; we would expect capacitance to become more sensitive to cell motions at higher frequencies (Lo et al., 1995).

3.1. Long-term correlations

We first examine correlations at long time scales. In the low-frequency limit, the power spectrum at the lower concentrations shows signs of long-time correlations, with the correlations getting weaker as the concentration is increased. A log–log plot of spectral density against frequency f suggests an intensity varying as $f^{-\alpha}$, with this trend becoming less clear at higher concentrations. We estimated α with least-squares straight-line fits of power from only the lowest 100 frequencies (excluding zero frequency and the next lowest frequency). For each run, we split the 2048 noise amplitudes into half-overlapping windows of 256 s, multiplied by a Hann window, Fourier transformed, and squared, averaging the resulting spectra in order to reduce scatter (Press et al., 1994).

Having obtained an α for every experiment, we then averaged these separately for each concentration. Our results are shown in Table 1, where $\bar{\alpha}$ is the average, σ_α is the standard deviation, and $\sigma_\alpha/\sqrt{N}$ the standard error of the mean, where N gives the number of experiments in the sample. The power α is also plotted against toxin concentration in Fig. S1 in the supplement to this paper. The first thing we notice in the table is that the means of the α s are separated by several standard errors ($\sigma/\sqrt{N}$). This implies that already with the power spectrum alone, given enough experiments, one could in principle distinguish the concentrations. More significantly, the means at concentrations of zero, 2.5, and 5.0 μM are separated from their neighboring means by at least a standard deviation σ; thus the power spectrum might be the strongest indicator for distinguishing different levels of this toxin in 3T3 fibroblasts. Although the mean values for α at every concentration in Table 1 are separated from those at every other concentration by at least a standard error, a version of the Student's t-test for non-equal-variance samples (Press et al., 1994, Eq. 14.2.3) shows a marginally insignificant (probability 11%) separation between the control and 0.1 μM populations. All other pairs of populations are significantly separated (probability <3%). The Kolmogorov–Smirnov test applied pairwise to the distribution of α values in each population gives the same result.

These power-slope averages also show a clear trend. As concentration increases, the power slope decreases. Thus, the long-term correlations, which are strongest at zero concentration, are disrupted by addition of the toxin.

There is a danger in looking only at power-law behavior to determine the existence of long-term correlations in time–series data (Rangarajan and Ding, 2000; Coronado and Carpena, 2005): white noise may mimic correlated (pink) noise in a short series. To guard against this problem, we look at two other indicators of long-term correlation, the exponents provided by rescaled range analysis (Hurst analysis) and detrended fluctuation analysis (Bassingthwaighte et al., 1994; Mandelbrot and Wallis, 1969; Feder, 1988; Peng et al., 1994, 1995). Both methods are binning techniques. A time series is split into bins of duration τ, and it is then determined how a measure $S(\tau)$ scales with τ. For Hurst, one subtracts the mean from all the data in a bin and characterizes that bin by its standard deviation, σ. The series is integrated, and the minimum value subtracted from the maximum, yielding the range, R. For each bin, one records the ratio R/σ and averages over bins of the same size. The procedure is repeated for successively larger bins (τ). A straight-line fit to a log–log plot of R/σ against bin size τ reveals a power law, $R/\sigma \sim \tau^H$, where H is the Hurst exponent. Detrended fluctuation analysis runs along similar lines, but within each bin one subtracts a best-fit line, thus detrending the data. The data in the bin are then characterized by standard deviation $\sigma \sim \tau^D$, where D is the DFA exponent.

Table 1 shows the results. $\bar{H}$ ($\bar{D}$) is the Hurst (DFA) exponent averaged over all experiments for each concentration. σ_i is the standard deviation and $\sigma_i/\sqrt{N}$ the standard error for measure $i = D, H$.

Neither Hurst nor DFA is as clear-cut as the power-spectrum analysis. For Hurst, concentrations that are close to each other overlap even when considering just the standard error. DFA is a little better, but using the standard error cannot distinguish zero concentration from 0.1 μM. Both Hurst and DFA show a decline in the exponents from the lowest concentration to the highest. That the overall separation seems to be better for DFA than for Hurst might be due to finite-size effects in the time series. As pointed out by Coronado and Carpena Coronado and Carpena (2005), DFA does a better job with finite time series than does Hurst. The Student's t-test seems to support this. While neither DFA nor Hurst differs significantly (t-test or Kolmogorov–Smirnov) among the three lowest concentrations of 0, 0.1, and 1 μM, the trends in these measures confirm the result of power-slope α, with the measures approaching their uncorrelated limits as concentration increases.

Moreover, Hurst and DFA can be used to validate power-spectral (α) results (Rangarajan and Ding, 2000). For purely correlated data,

Table 1
Long-term correlation. Power-spectral, Hurst, and DFA measures of confluent layers of 3T3 fibroblast resistive noise series averaged over all runs at different concentrations of the toxin cytochalasin B.

Concentration	N	$\bar{\alpha}$	σ_α	$\sigma_\alpha/\sqrt{N}$	$\bar{H}$	σ_H	$\sigma_H/\sqrt{N}$	$\bar{D}$	σ_D	$\sigma_D/\sqrt{N}$
0.0	9	0.854	0.102	0.034	0.764	0.062	0.020	0.832	0.036	0.012
0.1	12	0.780	0.097	0.028	0.768	0.038	0.011	0.837	0.045	0.013
1.0	12	0.664	0.131	0.038	0.746	0.045	0.013	0.787	0.035	0.010
2.5	10	0.400	0.104	0.033	0.690	0.032	0.010	0.706	0.032	0.010
5.0	11	−0.283	0.361	0.109	0.693	0.074	0.022	0.558	0.052	0.016
10.0	10	−0.843	0.463	0.147	0.605	0.118	0.037	0.403	0.107	0.034

The first and second columns give the concentration in μM and the number (N) of independent experiments. Shown are estimates for $1/f^\alpha$ behavior (α), Hurst (H), and detrended fluctuation analysis (D) exponents at low frequencies. The means of the α values differ by many standard errors of the mean ($\sigma/\sqrt{N}$, where σ is the standard deviation), allowing us to distinguish the populations composed of N runs just from the power spectrum. Notice that for the power spectrum, concentrations of zero, 2.5, and 5.0 μM are separated by σ, the standard deviation.

the Hurst exponent is fixed by α: $H = (1+\alpha)/2$. However, finite-size effects can lead to artificially large values for α, which an incompatible Hurst or DFA exponent can expose. We repeated the technique we introduced in Lovelady et al. (2007, Fig. 4), computing discrepancies between the values for both Hurst and DFA predicted from the numerical estimates for α and those measured in the time series. As in the previous work, the experimental discrepancies between α and DFA or Hurst were more consistent with those measured in artificial time series constructed to have long-time correlations than with the larger discrepancies of artificial white noise.

3.2. Short-term correlations

In order to investigate the short-term correlations in these systems, we look at the first zero and first $1/e$ crossings of the autocorrelation function. Our results are shown in Table S1 in the supplement. The $1/e$ crossing can distinguish zero concentration from 2.5 μM and 2.5 μM from 5.0 μM using the standard deviation, while the first zero crossing can do so with the standard error of the mean. Student's *t*-test confirms the significance of the $1/e$ crossing for distinguishing concentrations $\geq 1\,\mu M$ from zero concentration.

The trend for the $1/e$ crossing supports our hypothesis that the system is becoming less correlated with higher concentration of the toxin, as displayed in Fig. S2 of the supplement. The zero crossing does not do nearly as well; it cannot distinguish any of the three lowest concentrations.

3.3. Measure space

Using our measures of long- and short-term correlations in the noise, we can construct a multidimensional space each axis of which represents one of our measures, and each experiment is then a point in this space. We construct such a space with the four dimensions α, D, H, and $1/e$ crossing, normalizing to unit variance.

We find the vector in this space that represents the average position for each concentration and then construct a sphere about each average position with radius given by the root mean square of the standard errors along the four axes. Dividing the distance between the average position of the populations at two concentrations by the sum of their radii measures roughly their separation, with a ratio larger than unity indicating good separation. Table S2 in the supplement compares the six spheres. Even those clusters that overlap under this criterion, such as the zero-concentration and 0.1-μM spheres, have separation parameters closer to unity than to zero, suggesting that longer data sets might separate the measurements more clearly.

In order to get some picture of what is happening in this four-dimensional space, we project onto a plane whose two axes maximize the variance, *i.e.*, the first two principal components (Hotelling, 1933). Fig. S3 in the supplement shows clustering of the different concentrations. For this principal-component analysis, we omitted the runs at 10 μM. Starting from the highest concentration, the clusters are distinct, but as the concentration is reduced, the clusters get closer together and begin to overlap.

4. Discussion

We previously demonstrated use of these statistical tools on electrical-noise measurements from ECIS to distinguish cancerous and non-cancerous human ovarian surface epithelial cells in culture (Lovelady et al., 2007). We have now used these same tools to differentiate toxin levels in cultures of 3T3 fibroblasts. We have observed that, as the toxin level is increased, the long-term correlations, as measured by the power spectrum, Hurst exponent, and detrended fluctuation analysis, decrease. In addition, the short-term correlations, as measured by the first zero and $1/e$ crossing of the autocorrelation function, decrease as the toxin level is increased. If we interpret these correlations as a description of the level of communication and cooperation between cells, then these measures are describing a system that is in some sense coordinated, that coordination being disrupted by addition of the toxin cytochalasin B. Eventually, as the toxin reaches a threshold, the system is unable to work together, and the measures approach values typical of random systems. For example, the Hurst exponent drops from 0.764 in the control runs, indicating correlation, toward the value of $1/2$ expected for white noise. At the highest concentrations, α appears to go negative; however, the log–log power-spectral plots also become harder to interpret, so we expect that longer runs would give $\alpha = 0$ (white noise). The loss of temporal correlation with increasing toxin concentration can be explained by the effects of cytochalasin B on the cytoskeleton (Shier and Mebs, 1990; Tanenbaum, 1978). As the cytochalasin B interferes with cell function, the ability of the cells to maintain tight cell junctions is disrupted. The power-spectral slope, α, detects physiological effects on the culture at a statistically significant level for concentrations of cytochalasin B as low as 1 μM (Table 1), while the non-overlapping standard errors hint at a possible result for a concentration of 0.1 μM. However, careful analysis of multidimensional measures has so far failed to confirm this.

Noise analysis of ECIS data can be used to test statistical–mechanical models of micromotion. Looking further, we envision a database of electrical (ECIS) characteristics, with the collection of noise measures for each cell type and environment (e.g., toxin) constituting a kind of fingerprint: this could open the door to further applications, including drug screening and environmental sensing.

Acknowledgment

This work was supported by a grant from NIH/NCI 1R03CA123621-01A1 (C.-M. Lo).

Appendix A. Supplementary Data

Supplementary data associated with this article can be found, in the online version, at doi:10.1016/j.bios.2008.09.033.

References

Bassingthwaighte, J.B., Liebovitch, L.S., West, B.J., 1994. Fractal Physiology. Oxford University Press, New York.
Bonder, E.M., Mooseker, M.S., 1986. J. Cell Biol. 102, 282–288.
Brischwein, M., Motrescu, E.R., Cabala, E., Otto, A.M., Grothe, H., Wolf, B., 2003. Lab Chip 3, 234–240.
Brown, S.S., Spudich, J.A., 1981. J. Cell Biol. 88, 487–491.
Charrier, L., Yan, Y., Nguyen, H.T.T., Dalmasso, G., Laboisse, C.L., Gerwitz, A.T., Sitaraman, S.V., Merlin, D., 2007. J. Biol. Chem. 282, 16948–16958.
Coronado, A.V., Carpena, P., 2005. J. Biol. Phys. 31, 121–133.
Earley, S., Plopper, G.E., 2008. Biochem. Biophys. Res. Commun. 366, 476–482.
Feder, J., 1988. Fractals. Plenum Press, New York.
Foissner, I., Wasteneys, G.O., 2007. Plant Cell Physiol. 48, 585–587.
Giaever, I., Keese, C.R., 1984. Proc. Natl. Acad. Sci. U.S.A. 81, 3761–3764.
Giaever, I., Keese, C.R., 1989. Physica D 38, 128–133.
Giaever, I., Keese, C.R., 1991. Proc. Natl. Acad. Sci. U.S.A. 88, 7896–7900.
Hartmann, C., Zozulya, A., Wegener, J., Galla, H.-J., 2007. Exp. Cell. Res. 313, 1318–1325.
Hotelling, H., 1933. J. Educ. Psychol. 24, 417–441.
Keese, C.R., Karra, N., Dillon, B., Goldberg, A.M., Giaever, I., 1998. In-Vitro Mol. Toxicol. 11, 183–192.
Lo, C.-M., Keese, C.R., Giaever, I., 1993. Exp. Cell. Res. 204, 102–109.
Lo, C.-M., Keese, C.R., Giaever, I., 1995. Biophys. J. 69, 2800–2807.
Lovelady, D.C., Richmond, T.C., Maggi, A.N., Lo, C.-M., Rabson, D.A., 2007. Phys. Rev. E 76, 041908.
Mandelbrot, B.B., Wallis, J.R., 1969. Water Resour. Res. 5, 321–340.
Ohmori, H., Toyama, S., Toyama, S., 1992. J. Cell Biol. 116, 933–941.

Peng, C.-K., Buldyrev, S.V., Havlin, S., Simons, M., Stanley, H.E., Goldberger, A.L., 1994. Phys. Rev. E 49, 1685–1689.
Peng, C.-K., Havlin, S., Stanley, H.E., Goldberger, A.L., 1995. Chaos 5, 82–87.
Press, W.H., Teukolsky, S.A., Vetterling, W.T., Flannery, B.P., 1994. Numerical Recipes in C: the Art of Scientific Computing, second corrected edition. Cambridge University Press, Cambridge.
Rangarajan, G., Ding, M., 2000. Phys. Rev. E 61, 4991–5001.
Saxena, N.K., Sharma, D., Ding, X., Lin, S., Marra, F., Merlin, D., Anania, F.A., 2007. Cancer Res. 67, 2497–2507.
Shier, W.T., Mebs, D. (Eds.), 1990. Handbook of Toxinology. Marcel Dekker, Inc., New York.
Tanenbaum, S.W. (Ed.), 1978. Biochemical and Cell Biological Aspects. Elsevier North-Holland Biomedical Press, Amsterdam.
Xiao, C., Luong, J.H., 2005. Toxicol. Appl. Pharm. 206, 102–112.